AN APPROACH TO THE MULTI-AXIS PROBLEM IN MANUAL CONTROL

By Captain Walter W. Harrington

AFFDL/FGD
Wright-Patterson AFB

SUMMARY

The multi-axis control problem is addressed within the context of the optimal pilot model. The problem is developed to provide efficient adaptation of the optimal pilot model to complex aircraft systems and real world, multi-axis tasks. This is accomplished by establishing separability of the longitudinal and lateral control problems subject to the constraints of multi-axis attention and control allocation. Control solution adaptation to the constrained single axis attention allocations is provided by an optimal control frequency response algorithm. An algorithm is developed to solve the multi-axis control problem. The algorithm is then applied to an attitude hold task for a bare airframe fighter aircraft case with interesting multi-axis properties.

INTRODUCTION

Applications of the optimal pilot model [3-20], as well as other human operator models, have generally been limited to single axis control tasks. Methods to predict important optimal pilot model parameters, such as attention allocation [32,31] and control frequency response [34], for complex aircraft systems and tasks are recent developments. In addition, automation of the control frequency response [31] and signal to noise ratio optimal pilot model iteration loops has been accomplished only in the last few years.

This paper presents a method to solve the multi-axis control problem which is suitable for complex aircraft systems and tasks. The method takes advantage of recent developments [30,31,32,34] to be fully predictive. The method furthermore takes advantage of conventional separability assumptions for the longitudinal and lateral axis systems to provide efficient adaptation of the optimal pilot model to multi-axis tasks.

SYMBOLS

a	Threshold
A_a	Augmented open loop dynamics matrix ($n_s \times n_s$)
A_p	Augmented open loop dynamics matrix containing control filter ($n_s \times n_s$)
$\bar{A}$	Augmented closed loop dynamics matrix ($n_s \times n_s$)
B_a	Augmented control distribution matrix ($n_s \times n_c$)
C_a	Augmented measurement distribution matrix ($n_m \times n_s$)
E	Expected value
E_a	Augmented disturbance distribution matrix ($n_s \times n_d$)
f	Fraction of attention
f_{TOT}	Total attention to task
F_a	Augmented feedback matrix ($n_c \times n_s$)
g_f	Gradient of total cost with respect to fraction of attention
G	Kalman filter gain matrix
J	Control cost
J_o	Scanning cost
L	Effective feedback matrix to unaugmented state system ($n_c \times n_x$)
n_c	Number of controls
n_d	Number of disturbances
n_m	Number of measurements

n_s	Number of states in augmented system
n_x	Number of states in unaugmented system
P_a	Riccati control gain matrix for augmented system ($n_s \times n_s$)
P_m	Motor noise to signal ratio
P_y	Measurement noise to signal ratio
Q	Measurement penalty matrix ($n_m \times n_m$)
R	Control rate penalty matrix ($n_c \times n_c$)
tr	Trace
T	Gaussian random input describing function approximation for a threshold nonlinear
$\underline{u}$	Pilot's control input, a vector of dimension n_c
$\underline{V}_m$	Autocovariance of motor noise, a vector of dimension n_c
$\underline{V}_y$	Autocovariance of measurement noise, a vector of dimension n_m
$\underline{w}$	A disturbance vector of Gaussian white noise, a vector of dimension n_d
$\underline{x}_a$	State of the augmented system, a vector of dimension n_s
Σ_a	State covariance matrix of the augmented system ($n_s \times n_s$)
$\underline{y}$	A vector of measurements available to the pilot, of dimension n_m
Σ	Riccati filter covariance matrix
τ	Pure time delay
ω_c	Control cutoff frequency
ω_N	Neuromuscular cutoff frequency
Ω_c	Control filter matrix

Subscripts

a	Augmented
p	Perceived

Superscripts

T	*Transpose*
*	Optimal
^	Estimated parameter

OPTIMAL PILOT MODEL

The optimal pilot model concept, developed by Kleinman, Baron, and Levison [3-20], has demonstrated success in modeling complex, time varying control tasks. The optimal pilot model is a mathematical construct designed to synthesize pilot control performance and behavior. The model is based on the assumption that the human operator will control a dynamic, stochastic system optimally subject to his inherent limitations. These limitations are considered to be

1. A time delay, representing cognitive, visual central processing, and neuromotor delays.

2. "Remnant" signals, divided into an observation noise to represent signal degradation due to work load, scanning effects, and signal thresholds, and a motor noise to represent random errors in executing the intended control.

3. A "neuromuscular lag" to represent neuromuscular dynamics.

The control commands are synthesized by a continuous linear equalization network which contains a full state optimal filter (Kalman filter), a full state optimal predictor, and a full state optimal feedback control law. The control law is derived for an augmented state system which results from introducing the neuromuscular lag by means of a control rate penalty. The structure of the model results from a suboptimal solution to a control problem involving a time delay and observation noise. The model is shown in Figure 1.

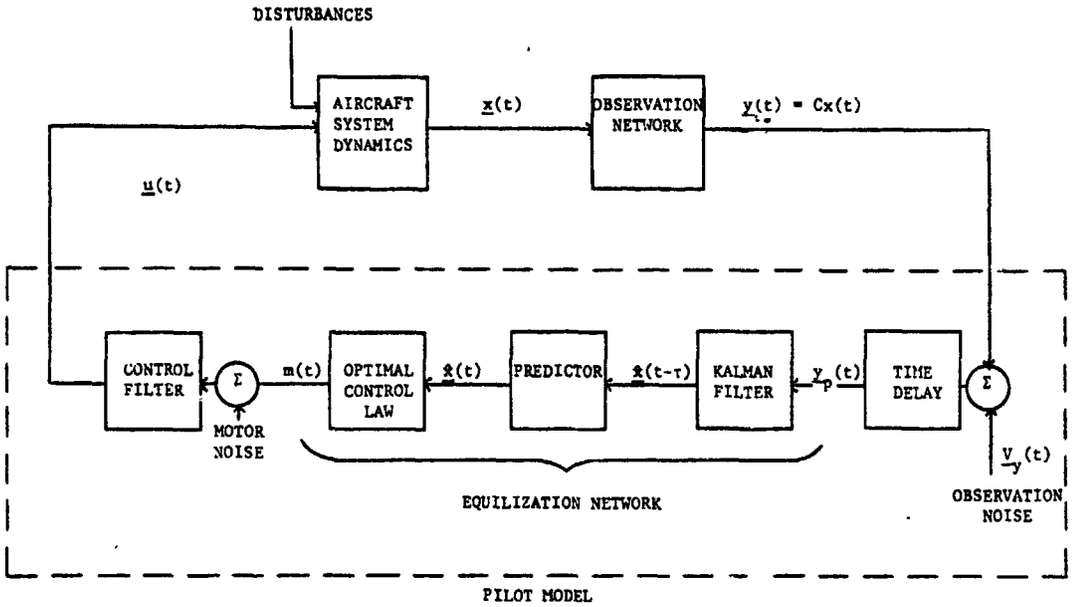

Figure 1 Structure of Optimal Pilot Model

The mathematical algorithm of the optimal pilot model is developed from the following control problem:

Given the quadratic cost functional of the form

$$J = 1/2 \int_0^\infty E\{\underline{y}^T(t)\, Q\, \underline{y}(t) + \underline{u}_a^T(t)\, R\, \underline{u}_a(t)\}\, dt \qquad (1)$$

subject to the constraints

$$\dot{\underline{x}}_a(t) = A_a \underline{x}_a(t) + B_a \underline{u}_a(t) + E_a \underline{w}_a(t) \qquad (2)$$

$$\underline{y}(t) = C_a \underline{x}_a(t - \tau) + \underline{V}_y(t - \tau), \qquad (3)$$

determine the non-anticipative feedback control $\underline{u}_a^*(t)$ which minimizes the cost functional.

Optimal Control Law

The optimal pilot model equalization network contains a full state optimal feedback control law. The pilot model determines the feedback control $\underline{u}_a^*(t)$ which minimizes the cost functional

$$J = \frac{1}{2} \int_0^\infty E\{\underline{y}^T(t) Q \underline{y}(t) + \underline{u}_a^T(t) R\, \underline{u}_a(t)\} dt \qquad (1)$$

subject to the constraints

$$\dot{\underline{x}}_a(t) = A_a \underline{x}_a(t) + B_a \underline{u}_a(t) \qquad (2a)$$

$$\underline{y}(t) = C_a \underline{x}(t) \qquad (3a)$$

by the solution of the steady state Riccati control matrix equation

$$A_a^T P_a + P_a A_a + C_a^T Q C_a - P_a B_a R^{-1} B_a^T P_a = 0 \qquad (4)$$

where

$$\underline{u}_a^*(t) = -R^{-1} B_a^T P_a \underline{x}_a(t).$$

The control law therefore requires the specification of the measurement penalty matrix Q and the control rate penalty matrix R. The measurement penalty matrix Q is specified to provide rms minimization of the measured quantities. The control rate penalty matrix R is related to control frequency response in the following section.

Control Frequency Response

Pilot control frequency is regulated in the optimal pilot model by a first order filter matrix which processes the augmented control signals such that

$$\underline{u}_a^*(t) = \dot{\underline{u}}(t) = -\Omega_c L\underline{x}(t) - \Omega_c \underline{u}(t) \tag{5}$$

It can be shown [31,34] that the filter matrix, Ω_c, is given by

$$\Omega_c = R^{-1} P_f \tag{6}$$

where

$$P_a = \left[\begin{array}{c|c} P & P_e \\ \hline P_c & P_f \end{array}\right] \tag{7}$$

is obtained from Equation (4).

The diagonal elements ω_{c_i}, i=1, ..., n_c, of Ω_c represent the first order cutoff frequencies of the control inputs u_i, i=1, ..., n_c. The cutoff frequencies are constrained such that

$$0 \le \omega_{c_i} \le \omega_{N_i}, \quad i=1, \ldots, n_c \tag{8}$$

where $\omega_{c_i} \ge 0$ by definition and ω_{N_i} is the pilot's neuromuscular frequency limit for the ith control input.

Iterative techniques have been developed [31] by which the control solution can be regulated so that the cutoff frequencies ω_{c_i}, i=1, ..., n_c, attain any desired set of values, subject to the constraints of Equation (8). These values can be predicted by the model through the optimal control frequency response algorithm [34]. This algorithm solves a complex, nonlinear optimization problem to determine the set of cutoff frequencies which minimize the cost function given by Equation (1) subject to the constraints of Equation (8). The algorithm normally forms an outer loop about the basic pilot model, requiring actual cost evaluation and optimization.

Full State Estimation

The optimal pilot model equalization network generates a full state estimate of the aircraft system based on noisy, delayed observations of the system. This estimate is the output of a Kalman filter. The filter gains are determined from the covariance matrix Σ which is the solution to the steady state Riccati filter equation

$$A_p\Sigma + \Sigma A_p^T + W - \Sigma C_a^T V_y^{-1} C_a \Sigma = 0 \tag{9}$$

where

$$W = E_a V_d E_a^T \tag{10}$$

The matrix V_d is the variance matrix of state disturbances of which the autocovariances of the motor noise, $\underline{V}_m$, are elements. Also,

$$\underline{V}_y = \text{Diagonal } (V_y) \tag{11}$$

where $\underline{V}_y$ is the autocovariance of the measurement noise. The filter therefore requires specification of the autocovariance of the measurement noise $\underline{V}_y$ associated with the measurements $\underline{y}(t)$ and the autocovariance of the motor noise $\underline{V}_m$ associated with the controls $\underline{u}(t)$.

Pilot Model Measurements

The optimal pilot model is well suited for realistic synthesis of human operator information processing. The pilot model can observe those instruments or quantities which the pilot would observe to perform the flight task. Furthermore, the pilot model contains algorithms for amplitude and rate information processing, attention allocation, and signal perception.

Measurement Noise

The optimal pilot model contains measurement noise to represent signal degradation due to work load, attention allocation, and signal thresholds. It is assumed that the covariance $\underline{V}_{y_i}$ of each measurement noise $v_{y_i}(t)$, $i=1, \ldots, n_m$, is given by

$$\underline{V}_{y_i} = \frac{\pi P_y}{f_i T^2} E\{y_i^2(t)\}, \quad i=1, \ldots, n_m \tag{12}$$

where P_y is the full attention noise to signal ratio,

$$P_y = .01, \tag{13}$$

f_i is the fraction of attention allocated to $y_i(t)$, subject to the constraints

$$\sum_{i=1}^{n_m} f_i = f_{TOT} \leq 1 \tag{14}$$

$$f_i \geq 0 \tag{15}$$

and T is a Gaussian input describing function approximation for a threshold of a_i,

$$T = \operatorname{erfc} \frac{a_i}{\sqrt{2}\,\sigma_i} \tag{16}$$

where $\sigma_i = \sqrt{E\{y_i^2(t)\}}$. Iteration of the covariance calculations is required since the autocovariance of the motor noise is a function of system performance. A method for predicting the attention allocation is presented in the following section.

Attention Allocation

An optimal attention allocation algorithm has been developed by Kleinman [32] to solve the optimal attention allocation problem. The basic hypothesis of optimal attention allocation is that the human pilot will adapt his attention allocation so as to minimize the cost functional given by Equation (1) subject to the constraints given by Equations (14) and (15). The optimization process developed by Kleinman is carried out numerically via a gradient algorithm which determines an unconstrained gradient vector, g_f. An optimization algorithm then solves the constrained optimization problem.

Motor Noise

The optimal pilot model contains motor noise to represent random errors in the execution of the intended control as well as control signal degradation due to work load and attention allocation. The autocovariance or the motor noise is given by [31]

$$\underline{V}_{m_i} = \frac{\pi P_m}{f_{TOT}} E\{u_i^2(t)\}, \quad i=1, \ldots, n_c \tag{17}$$

where P_m is the full attention allocation noise to signal ratio,

$$P_m = .003 \tag{18}$$

and f_{TOT} is the total attention to the task. The autocovariance of the motor noise completes the specification of quantities required by the Kalman filter.

Full State Prediction

The optimal pilot model equalization network contains an optimal, full state predictor which updates the delayed full state estimate generated by the Kalman filter. It is required by the predictor to specify the pure time delay τ by which the observations $\underline{y}(\tau)$ are delayed.

Pilot Model Performance Prediction

The optimal pilot model synthesizes pilot control performance by the generation of piecewise constant aircraft system statistics. The state covariance matrix X arises from the sum of the covariance of the filter estimate, the covariance of the estimation error, and the covariance of the predictor error [8]. Thus,

$$X = E\{\underline{x}_a(t)\,\underline{x}_a^T(t)\} \tag{19}$$

$$= \int_0^\infty e^{\bar{A}\sigma} e^{A_p\tau}\,\Sigma\, C_a V_y^{-1} C_a \Sigma e^{A_p^T\tau} e^{\bar{A}\sigma} d\sigma$$

$$+ e^{A_p\tau}\,\Sigma\, e^{A_p^T\tau} + \int_0^\tau e^{A_p\sigma} W e^{A_p^T\sigma} d\sigma$$

The standard deviation of the aircraft states is then given by

$$\sigma_{x_i} = \sqrt{E\{x_i^2(t)\}} = \sqrt{(X)_{ii}} \tag{20}$$

The standard deviation of the measurements is given by

$$\sigma_{y_i} = \sqrt{(C_a X C_a^T)_{ii}} \tag{21}$$

In addition to the rms statistics, the optimal pilot model has predicted the control frequency response and attention allocation. Pilot ratings [29] can also be predicted.

APPLICATION OF THE OPTIMAL PILOT MODEL TO COMPLEX AIRCRAFT SYSTEMS AND MULTI-AXIS TASKS

Typical aircraft systems contain many subsystems, including a control feel system, control actuators, the bare airframe, a stability augmentation system, and instrument and visual display systems. Since the optimal pilot model requires a linear representation of the aircraft system dynamics, these subsystems must be represented by sets of first order, linearized, piecewise constant coefficient, differential equations of motion. Statistical linearization techniques can be applied to nonlinearities. Iteration is then required to adapt these coefficients to the resulting system performance.

The resulting state model of the aircraft system dynamics can be quite large, requiring excessive time and core requirements for computer implementation of the optimal pilot model. However, several considerations can result in significant reduction of these requirements.

Decoupling of the Optimal Control Law

The linearized representation of conventional aircraft systems results in decoupled sets of longitudinal and lateral equations. If the pilot does not intentionally couple the longitudinal and lateral axis systems, i.e., Ω and R are block diagonal in a manner similar to the decoupling of the system equations, the control problem formed by seeking the feedback control $\underline{u}^*(t)$, which minimizes J subject to the constraints of Equations (2a) and (3a), decouples into two separate control problems. The measurement penalty matrix Q is normally specified to be diagonal, which of course satisfies the constraint of being block diagonal. In addition, the control rate penalty matrix R is normally specified to be diagonal for the control frequency response regulation algorithm [31]. Thus, the control law can be determined for each axis system for multi-axis tasks.

Control Frequency Response

Control frequency response, as specified by the optimal control frequency response algorithm [31,34], is dependent upon predicted system performance. However, the assumptions of the previous section imply that the control filter matrix, Ω_c, given by Equation (6) is block diagonal. Thus, if the covariance propagation problem can be constrained for each axis system, the optimal control frequency response problem decouples into two separate control problems.

Full State Estimation

The separability of the state estimation problem is dependent upon the specification of the state disturbances and measurement noise. The state disturbances, including the motor noise, are usually model by independent Gaussian white noise sources, which are separable. It is proposed that f_{TOT} in Equation (17)

$$\underline{V}_{m_i} = \frac{\pi P_m}{f_{TOT}}\, E\{u_i^2(t)\},\ i=1,\ \ldots,\ n_c \tag{17}$$

be represented by the total attention allocation for each axis system. The uncertainty of control is then related to the attention to control for each axis system.

The measurement noises are decoupled for each axis system with the exception of dependence upon attention allocation. Thus, the state estimation problem is coupled by the attention allocation algorithm.

Attention Allocation

The optimal attention allocation algorithm developed by Kleinman [32] has two major components: the gradient algorithm which determines an unconstrained gradient vector, and the optimization algorithm which solves the constrained optimization problem. The gradient algorithm is decoupled for each axis system. However, the optimization problem must be solved for the entire aircraft system.

If the total attention allocation is constrained for each axis system for each attention optimization iteration, the state estimation problem can be decoupled. The optimal attention allocation gradient algorithm can then be applied separately to each axis system. The optimal attention allocation optimization algorithm is then applied to the entire system. Note that the optimization algorithm should not be applied to each axis system, since this will only identify local minima, as well as incur additional computation cost.

Covariance Propagation

The remaining covariance propagation problems are decoupled into the longitudinal and lateral axis systems. If the attention allocation is constrained for each axis system for each attention optimization iteration as described in the previous section, the covariance propagation problem is also constrained, as required for decoupling of the optimal control frequency response problem. Note that the attention allocation optimization algorithm now forms an outer iteration loop about the optimal control frequency response algorithm. This is satisfactory since the two algorithms are mutually adaptive to each other.

Computation Requirements

The multi-axis control problem can be decoupled into the longitudinal and lateral control problems with the exception of attention allocation optimization. The separate solution of longitudinal and lateral control problems will require much less computation time due to the reduction in matrix size. Furthermore, the same core can be used for both solutions. Thus, significant time and core savings can be realized by this approach.

Flow charts of the computations required by this approach are shown in Figures 2 and 3. The computations are structured so as not to interfere with the utility of the model for single axis tasks. The multi-axis attention optimization, as well as storage of required pilot model parameters, is therefore performed by a separate subroutine.

APPLICATION TO AN ATTITUDE HOLD TASK

The multi-axis control task scheme is applied to an attitude hold task for a bare airframe fighter aircraft case. An attitude hold task for a bare airframe provides a simple example which can be easily duplicated for further research in this area. The bare airframe fighter aircraft case selected has unstable longitudinal dynamics and more conventional lateral dynamics, which will be useful for the illustration of basic properties of the multi-axis control task scheme.

Aircraft System

The fighter aircraft case involves straight and level flight at an altitude of 3,048 meters (10,000 feet) at an airspeed of 262 meters/second (862 feet/second). The airframe dynamics for this case are modeled by standard, linearized, primed, longitudinal and lateral body axis equations of motion [31]. The stability derivatives and other parameters pertinent to this case are presented in Table 1. For simplicity, as well as to accentuate the aircraft dynamics, no models are included for the stability augmentation system or control feel system. The airframe is disturbed by turbulence with gust intensities of 5 feet/second. MIL SPEC 8785B turbulence is provided, as modeled by Heath [24].

Controls include a side stick for pitch and roll and pedals for yaw. The neuromuscular frequency response limits are estimated to be 10, 10, and 5 radians/second for the pitch stick, roll stick, and pedals, respectively [25,26]. The multi-dimensional control for the lateral axis system will be useful to demonstrate the utility of the multi-axis control task algorithms.

Measured quantities include pitch angle, vertical velocity, roll angle, and yaw angle. It is assumed that the rates of these quantities are simultaneously available. The perceptual thresholds for the measured quantities are presented in Table 2.

Task

The task is defined to be precision attitude hold in turbulence. Control action is required as soon as a deviation in measured quantities is noticed, and deviations must be maintained within specified limits. A total of 80% attention is allocated to this task.

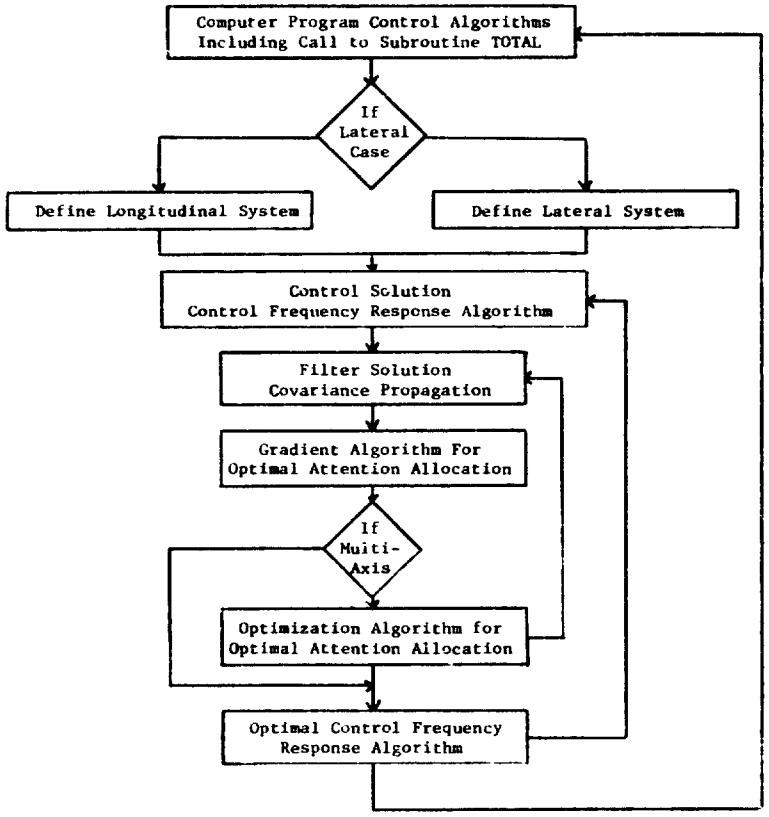

Figure 2. Main Program Structure for Multi-Axis Problem

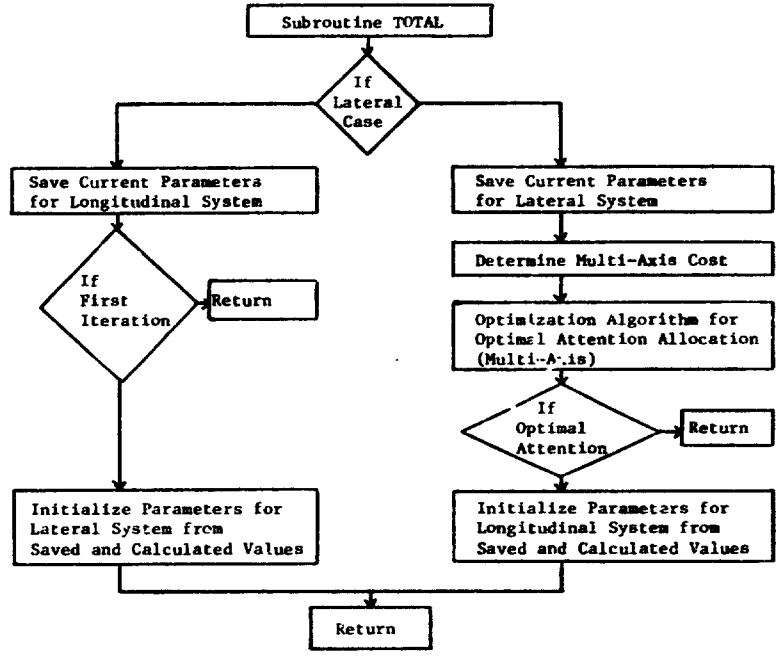

Figure 3. Subroutine TOTAL Structure for Multi-Axis Problem

PARAMETER	LONGITUDINAL AXIS SYSTEM	LATERAL AXIS SYSTEM
Unprimed Stability Derivatives	X_u = -.01578 X_w = .02144 $X_{\delta e}$ = 20.6 M_u = -.001169 M_w = .005766 M_q = -.6528 $M_{\delta e}$ = -28.2 $M_{\dot{w}}$ = -.0003094 Z_u = -.06086 Z_w = -1.692 $Z_{\delta e}$ = -157.3	Y_v = -.2932 $Y_{\delta a}$ = 14.15 $Y_{\delta r}$ = 50.72 L_β = -70.95 L_p = -2.551 L_r = -.06964 $L_{\delta a}$ = -62.92 $L_{\delta r}$ = 17.01 N_β = 11.51 N_p = -.01704 N_r = -.2266 $N_{\delta a}$ = -2.261 $N_{\delta r}$ = -9.057
Moments		I_{xx} = 9017.5 I_{zz} = 58104. I_{xz} = 144.93
Wing Span	30.	30
Total Velocity	862.0	862.0
Flight Path Angle	0.	0.
Angle of Attack	1.5285	1.5285
Altitude	10000.	10000.
Units	Feet, Seconds, Radians	Feet, Seconds, Radians

TABLE 1. FIGHTER AIRCRAFT STABILITY DERIVATIVES AND OTHER PARAMETERS

MEASURED QUANTITY	UNITS	PERCEPTUAL THRESHOLD	INDIFFERENCE THRESHOLD	MAXIMUM ALLOWABLE DEVIATION	STATE PENALTY
Pitch Angle	deg.	.8	.8	10.	.01
Pitch Rate	deg./sec.	1.6	1.6	32.	.001
Vertical Velocity	ft./sec.	.27	.27	10.	.01
Vertical Acceleration	ft./sec.^{2}	.54	.54	32.	.001
Roll Angle	deg.	.9	.9	10.	.01
Roll Rate	deg./sec.	1.8	1.8	32.	.001
Yaw Angle	deg.	.9	.9	10.	.01
Yaw Rate	deg./sec.	1.8	1.8	32.	.001

Table 2. Measured Quantities and Related Parameters

Immediate control action implies that the indifference thresholds are the same as the perceptual thresholds, as presented in Table 2. The maximum allowable deviations are also presented in this table. The optimal pilot model state penalties are derived by the conventional rule

$$Q_{ii} = \left(\frac{1}{\text{MAX}|y_i(t)|} \right)^2 \qquad (31)$$

and are presented in Table 2.

Model Predictions

The multi-axis control task scheme is implemented on the AFFDL optimal pilot model computer program NGDPILOT [31], which is designed for complex aircraft system and simulation analysis. The computer program is completely automated, and requires essentially only those parameters presented in this section. The program contains nominal values for all the basic optimal pilot model parameters. Program predictions include optimal control frequency response, optimal attention allocation [32], control and aircraft system performance, and pilot rating [29]. Predictions for this case are presented in Figure 4.

The predicted attention allocation for this case is presented in Table 3. This attention allocation is shown in comparison with the single axis results obtained in reference [34], where 40% attention was allocated to each axis system. The multi-axis solution indicates a large shift in attention allocation to the unstable longitudinal axis system, as would be expected.

OBSERVED QUANTITY	SINGLE AXIS ATTENTION ALLOCATION	TOTAL SINGLE AXIS ATTENTION ALLOCATION	MULTI-AXIS ATTENTION ALLOCATION	TOTAL MULTI-AXIS ATTENTION ALLOCATION
Pitch Angle	.031		.200	
Pitch Rate	.031	.400	.200	.697
Vertical Velocity	.369		.497	
Vertical Accel	.369		.497	
Roll Angle	.304		.086	
Roll Rate	.304	.400	.086	.103
Yaw Angle	.096		.017	
Yaw Rate	.096		.017	

Table 3. Predicted Attention Allocation


```
CASE DESCRIPTION

BARE AIRFRAME DYNAMICS, M=.8
6-DOF PRECISION ATTITUDE HOLD TASK WITH PITCH STICK, ROLL STICK AND PEDALS
LONGITUDINAL DYNAMICS

ALTITUDE = 1.000000E+04 FEET
NOMINAL AIRSPEED = 8.616933E+02 FEET/SECOND
NOMINAL ANGLE OF ATTACK = 1.528500E+00 DEGREES
TURBULENCE CONDITIONS
     SIG U GUST = 5.000000E+00 FEET/SECOND
     SIG V GUST = 5.000000E+00 FEET/SECOND
     SIG W GUST = 5.000000E+00 FEET/SECOND

AIRFRAME EIGENVALUES
(-3.668128 3)+J(0.)
(1.085537 7)+J(0.)
(-.22298678E-01)+J(.13527864)
(-.22298678E-01)+J(-.13527864)

                    PILOT MODEL PARAMETERS

TOTAL ATTENTION ALLOCATION TO PRIMARY FLIGHT TASK (ATTN) = .696898E+00
PURE TIME DELAY (TAU) = .200000E+00 SECONDS
MOTOR NOISE TO SIGNAL RATIO (PY) = 1.000000E-02
TOTAL COST (COST) = 1.285988E+00
SCANNING COST (SCOST) = 8.281187E-01
```

Figure 4. Optimal Pilot Model Performance Predictions for Multi-Axis F-16 Bare Airframe Attitude Hold Task (1 of 4)

CONTROLS

CONTROLLER	NEUROMUSCULAR FREQUENCY	OPTIMAL CONTROL FREQUENCY	CONTROL RATE PENALTY (RINV)	CONTROL FORCE STD DEVIATION	CONTROL SURFACE STD DEVIATION
PITCH STICK	10.000000	10.317287	9.9196789	.2145517	.21455517

OBSERVED QUANTITIES

OBSERVED QUANTITY	UNITS	TASK VECTOR	PERCEPTUAL THRESHOLD	INDIFFERENCE THRESHOLD	ATTENTION ALLOCATION	STANDARD DEVIATION
PITCH ANGLE	DEG	.10000000E-01	.80000000	.80000000	.19969588	3.5283864
PITCH RATE	DEG/SEC	.10000000E-02	1.6000000	1.6000000	.19989588	1.4511777
VERTICAL VELOCITY	FT/SEC	.10000000E-01	.27000000	.27000000	.49700244	7.1923670
VERTICAL ACCEL	FT/SEC**2	.10000000E-02	.54000000	.54000000	.49700244	21.733312

Figure 4. Optimal Pilot Model Performance Predictions for Multi-Axis F-16 Bare Airframe Attitude Hold Task (2 of 4)

CASE DESCRIPTION

BARE AIRFRAME DYNAMICS, M = .8
6-DOF PRECISION ATTITUDE HOLD TASK WITH PITCH STICK, ROLL STICK AND PEDALS
LATERAL DYNAMICS

ALTITUDE = 1.000000E+04 FEET
NOMINAL AIRSPEED = 8.616933E+02 FEET/SECOND
NOMINAL ANGLE OF ATTACK = 1.528500E+00 DEGREES
TURBULENCE CONDITIONS
SIG U GUST = 5.000000E+00 FEET/SECOND
SIG V GUST = 5.000000E+00 FEET/SECOND
SIG W GUST = 5.000000E+00 FEET/SECOND

AIRFRAME EIGENVALUES
(0.)+J(0.)
(-2.5341997)+J(0.)
(-.1876088E-01)+J(3.6290849)
(-.25919919)+J(-3.6290849)

PILOT MODEL PARAMETERS

TOTAL ATTENTION ALLOCATION TO PRIMARY FLIGHT TASK (ATTN) = .103102E+00
PURE TIME DELAY (TAU) = .200000E+00 SECONDS
MOTOR NOISE TO SIGNAL RATIO (PM) = 3.000000E-03
MEASUREMENT NOISE TO SIGNAL RATIO (PY) = 1.000000E-02
TOTAL COST (COST) = 3.528117E-01
SCANNING COST (SCOST) = 1.290835E-01

Figure 4. Optimal Pilot Model Performance Predictions for Multi-Axis F-16 Bare Airframe Attitude Hold Task (3 of 4)

The predicted control frequency responses for this case are presented in Table 4. These results are shown in comparison with the results obtained in reference [34]. The maximum physically attainable frequency response is again predicted for the unstable longitudinal axis system. But, a substantial reduction in control frequency response is predicted for the lateral axis system. This reduction is most consistent with the reduction in attention allocation to this axis system. Note that the pedal cutoff frequency of .2 radians/second corresponds to a control cycle time of about 30 seconds. These values could not be predicted by previous methods.

CONTROLLER	NEUROMUSCULAR CUTOFF FREQUENCY	SINGLE AXIS OPTIMAL CONTROL CUTOFF FREQUENCY	MULTI-AXIS OPTIMAL CONTROL CUTOFF FREQUENCY
Pitch Stick	10.rad/sec	10.rad/sec	10.rad/sec
Roll Stick	10.rad/sec	7.6rad/sec	4.2rad/sec
Pedals	5.rad/sec	4.4rad/sec	.20rad/sec

Table 4. Predicted Control Frequency Response

The multi-axis solution also produces a substantial reduction in total quadratic cost, as shown in Table 5. This is further evidence of the adaptive capability of the methods developed herein and in reference [34].

AXIS SYSTEM	SINGLE AXIS QUADRATIC COST	MULTI-AXIS QUADRATIC COST
Longitudinal	2.51	1.29
Lateral	.18	.35
TOTAL SYSTEM	2.69	1.64

Table 5. Predicted Quadratic Cost

SUMMARY OF THE MULTI-AXIS CONTROL PROBLEM

A method has been presented to efficiently solve the multi-axis control problem which is suitable for complex aircraft systems and

Figure 4. Optimal Pilot Model Performance Predictions for Multi-Axis F-16 Rare Airframe Attitude Hold Task (4 of 4)

CONTROLS

CONTROLLER	NEUROMUSCULAR FREQUENCY	OPTIMAL CONTROL FREQUENCY	CONTROL RATE PENALTY (RINV)	CONTROL FORCE STD DEVIATION	CONTROL SURFACE STD DEVIATION
ROLL STICK	10.00000	4.150179	11.98697	.2093625	.2093625
PEDALS	5.000000	.2026449	.4535230	.2495647	.2495647

OBSERVED QUANTITIES

OBSERVED QUANTITY	UNITS	TASK VECTOR	PERCEPTUAL THRESHOLD	INDIFFERENCE THRESHOLD	ATTENTION ALLOCATION	STANDARD DEVIATION
ROLL ANGLE	DEG	.1000000E-01	.9000000	.9000000	.8576538E-01	4.407269
ROLL RATE	DEG/SEC	.1000000E-02	1.800000	1.800000	.8576538E-01	10.88896
YAW ANGLE	DEG	.1000000E-01	.9000000	.9000000	.1733609E-01	1.249487
YAW RATE	DEG/SEC	.1000000E-02	1.800000	1.800000	.1733609E-01	2.403652

tasks. The method has been applied to an attitude hold task for a bare airframe fighter aircraft case. This application demonstrated the method's capability to make realistic predictions for stable as well as unstable aircraft system dynamics and for scalar as well as multi-dimensional controls. The method shows great promise for complex aircraft system and simulation analysis.

REFERENCES

1. Gressang, Stone, Pollard, and Kugel: Low Visibility Landing Pilot Modeling Experiment and Data, Phase I. AFFDL TR 75-41, April 1976.

2. Gressand: Low Visibility Landing Pilot Modeling Experiments and Data, Phase II. AFFDL TR 75-57, August 1975.

3. McRuer and Krendel: Mathematical Models of Human Pilot Behavior. AGARDograph No. 188, January 1974.

4. Baron and Kleinman: The Human As An Optimal Controller and Information Processor. IEEE Trans. Man-Machine Systems, Vol. MMS-10, March 1969, pp 9 - 17.

5. Baron et al: Application of Optimal Control Theory to the Prediction of Human Performance In A Complex Task. AFFDL TR 69-81, March 1970.

6. Kleinman, Baron, and Levison: A Control Theoretic Approach to Manned-Vehicle Systems Analysis. IEEE Trans. Auto. Control, Vol. AC-16, December 1971, pp 824-832.

7. Kleinman, Baron, and Levison: An Optimal-Control Model of Human Response, Part I: Theory and Validation. Automatica, Vol. 6, 1970, pp 357-369.

8. Kleinman: Optimal Control of Linear Systems with Time-Delay and Observation Noise. IEEE Trans. Auto. Control, Vol. AC-14, October 1969, pp 524-527.

9. Graham and McRuer: Analysis of Nonlinear Control Systems. Dover Publications, New York, 1971, Chapter 6.

10. Baron and Levison: An Optimal Control Methodology for Analyzing the Effects of Display Parameters On Performance and Work Load in Manual Flight Control. IEEE Trans. on Systems, Man, and Cybernetics, Vol. SMC-5, July 1975, pp 423-430.

11. Bryson and Ho: Applied Optimal Control. Ginn and Co., Waltham, Mass., 1969, Chapter 5.

12. Kleinman and Baron: Analytic Evaluation of Display Requirements for Approach to Landing. NASA CR-1952, October 1971.

13. Kleinman and Perkins: Modeling Human Performance in a Time-Varying Anti-Aircraft Tracking Loop. IEEE Trans. Auto. Control, Vol AC-19, August 1974, pp 297-306.

14. Harvey: Application of An Optimal Control Pilot Model to Air-to-Air Combat. AFIT Thesis GA/MA/74M-1, March 1974.

15. Dillow, Picha and Anderson: Slushy Weightings for the Optimal Pilot Model. 11th Annual Conference on Manual Control, May 1975.

16. Kleinman: Computer Programs Useful in Linear Systems Studies. Systems Control, Inc., Technical Memorandum, December 1971.

17. Kleinman: On An Iterative Technique for Riccati Equation Computation. IEEE Trans. Auto. Control, Vol. AC-13, February 1968, pp 114-115.

18. Kwakernaak and Sivan: Linear Optimal Control Systems. John Wiley, New York, 1972, Chapter 3.

19. McRuer, Ashkenas, and Graham: Aircraft Dynamics and Automatic Control. Princeton University Press, 1973, Chapters 5 and 6.

20. Kleinman and Killingsworth: A Predictive Pilot Model for STOL Aircraft Landing. NASA CR-2374, March 1974.

21. Gressang: A Note on Solving Riccati Equations Associated with Optimal Pilot Models. AFIT/AIAA Mini Symposium on Recent Advances in Aeronautical Research Development, and Systems, WPAFB, 26 March 1975.

22. Bryson and Hall: Optimal Control and Filter Synthesis by Eigenvector Decomposition. Report, Dept. of Aero. and Astro., Stanford University, December 1971.

23. McRuer and Graham: Human Pilot Dynamics in Compensatory Systems. AFFDL TR 69-72, July 1965.

24. Heath: State Varible Model of Wind Gusts. AFFDL/FGC TM-72-12, July 1972.

25. Stark: Neurological Control Systems, Studies in Bioengineering. Plenum Press, New York, 1968.

26. Milsum: Biological Control Systems Analysis. McGraw-Hill Book Company, New York, 1966.

27. Curry, Young, Hoffman, and Kugel: A Pilot Model with Visual and Motion Cues. AIAA Visual and Motion Simulation Conference, Dayton, Ohio, April 1976.

28. Harrington: The Application of Pilot Modeling to the Study of Low Visibility Landing. Twelfth Conference on Manual Control, May 1976.

29. Hess: Prediction of Pilot Opinion Ratings Using An Optimal Pilot Model. To appear in Human Factors.

30. Curry, Hoffman, Young: Pilot Modeling for Manned Simulation. AFFDL-TR-76-124, Volume I, December 1976.

31. Harrington: A Computer Program for the Analysis of Manned Aircraft and Simulation Systems. AFFDL TR to be published.

32. Kleinman: Solving the Optimal Attention Allocation Problem in Manual Control. IEEE Trans. Auto. Control, Vol. AC-21, No. 6, December 1976, pp 813-821.

33. Hoffman, Curry, Kleinman, Hollister, Young: Display/Control Requirements for VTOL Aircraft. ASI-TR-75-26 (NASA CR 145026), August 1975.

34. Harrington. The Optimal Control Frequency Response Problem in Manual Control. Thirteenth Conference on Manual Control, June 1977.